J. Plasma Physics (2002), *vol.* 67, *part* 4, *pp.* 243–250.
DOI: 10.1017/S0022377802001691 Printed in the United Kingdom

The floating potential of spherical probes and dust grains. Part 1. Radial motion theory

R. V. KENNEDY and J. E. ALLEN

Oxford University, Department of Engineering Science, Parks Road, Oxford OX1 3PJ, UK

(Received 14 September 2001)

Abstract. A theoretical analysis of spherical probes in plasmas is presented. It is assumed that the probe is at floating potential, that ion motion with respect to the probe is radial and that the electrons are Maxwellian. The analysis shows that as probe radius divided by Debye length tends to zero, the ratio of floating potential to electron temperature also goes to zero.

1. Introduction

Interactions between dust and plasma are common in a wide variety of situations. Dusty plasmas are observed in space, where they are found in interstellar and circumstellar clouds, planetary rings and magnetospheres and comets (Northrop 1992; de Angelis 1992). In industrial plasmas, dust occurs as a contaminant to be removed, while numerous experimental studies of dust behaviour have been undertaken. Applications for dusty plasmas include powder and thin-film synthesis, as described by Bouchoule (1999). Wherever dust is exposed to plasma, it becomes electrically charged. The potential of dust grains in plasmas is described in the literature by models that treat a single dust grain as a spherical probe at floating potential. There have been two main approaches to the collection of ions by a spherical probe. Orbital motion theory applies where ion temperature is significant (see Bohm et al. (1949) and Bernstein and Rabinowitz (1959) for monoenergetic ions and Laframboise (1966) for the Maxwellian case). The radial motion theory of Allen et al. (1957) (ABR) is valid where ion temperature is much smaller than electron temperature. In this paper, the radial theory is examined in the limit of small probe radius.

2. The radial motion theory

Consider a spherical probe immersed in a plasma as shown in Fig. 1. Far from the surface, the electrons and ions (singly charged) are equal in density. The surface potential V_p is unknown, but the total current at the surface is zero.

An ion at distance r from the centre of the probe moves towards it at speed u_i. Assume that the ion started at an infinite distance with no kinetic energy, and that the ions are collisionless, so

$$\tfrac{1}{2}M_i u_i^2 = -eV(r), \tag{1}$$

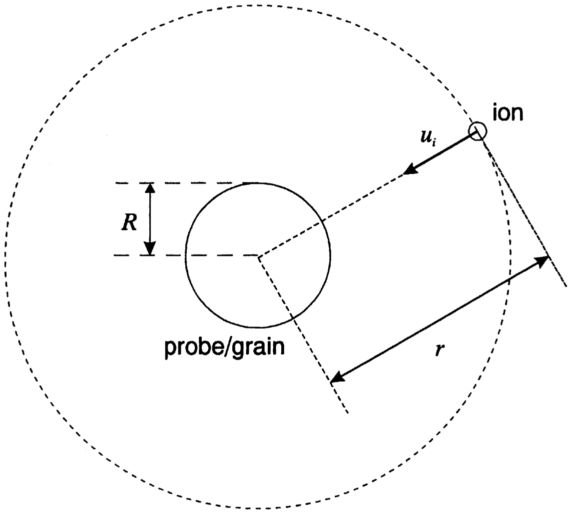

Figure 1. Schematic of a spherical probe.

where $V(r)$ is the potential at this radius, which vanishes as $r \to \infty$. Poisson's law can be expressed as

$$\nabla^2 V = -\frac{\text{charge density}}{\varepsilon_0} = -\frac{1}{\varepsilon_0} e(n_i - n_e), \tag{2}$$

where n_i and n_e are the ion and electron densities, e is the charge magnitude of an electron and ε_0 is the permittivity of free space. The (as yet unknown) ion current I_i is related to the local ion density and speed:

$$I_i = n_i(r) e u_i(r) 4\pi r^2$$

$$\Longrightarrow n_i(r) = \frac{I_i}{4\pi r^2 e u_i(r)}. \tag{3}$$

If relatively few electrons reach the probe, the electron density follows a Boltzmann relation:

$$n_e(r) = n_0 \exp\left(\frac{eV}{kT_e}\right), \tag{4}$$

where T_e is the electron temperature, k is the Boltzmann constant and n_0 is the plasma density. Assuming a perfectly absorbing surface, the actual electron density is likely to be smaller than that given by (4) because those electrons that hit the surface will only contribute to the density on their inbound trajectory, whereas those that do not will have both positive and negative radial velocities at different times. This electron depletion will be most marked close to the probe surface, where n_e approaches half of the given value. However, we expect (4) to be a good approximation over most of the sheath.

The electron flux to the surface is obtained by integrating the radial velocity over velocity space, but considering only the inbound electrons, which are unaffected by the above mentioned depletion. Multiplying by surface area and electron charge, and neglecting secondary emission and photoemission, we obtain the surface

https://doi.org/10.1017/S0022377802001691 Published online by Cambridge University Press

electron current as

$$I_i = I_e = 4\pi R^2 n_0 e \sqrt{\frac{kT_e}{2\pi m_e}} \exp\left(\frac{eV_p}{kT_e}\right). \tag{5}$$

It is convenient to normalize as follows:

$$\left.\begin{aligned} \phi &= -\frac{eV}{kT_e}, \qquad \rho = \frac{r}{\lambda_D}, \qquad P = \frac{R}{\lambda_D}, \\ N_i &= \frac{n_i}{n_0}, \qquad N_e = \frac{n_e}{n_0}, \qquad J = \frac{I_i}{n_0 e\sqrt{2kT_e/M_i}4\pi\lambda_D^2}, \end{aligned}\right\} \tag{6}$$

where λ_D is the electron Debye length, given by

$$\lambda_D = \sqrt{\frac{\varepsilon_0 kT_e}{n_0 e^2}}. \tag{7}$$

Substituting (6) and (7) into (2) with spherical symmetry gives

$$\frac{1}{\rho^2}\frac{d}{d\rho}\left(\rho^2 \frac{d\phi}{d\rho}\right) = N_i - N_e. \tag{8}$$

The normalized densities from (3) and (4) are $N_i = J\phi^{-1/2}/\rho^2$ and $N_e = \exp(-\phi)$. Substituting these into (8) gives

$$\frac{d}{d\rho}\left(\rho^2 \frac{d\phi}{d\rho}\right) = J\phi^{-1/2} - \rho^2 e^{-\phi}. \tag{9}$$

This is integrated numerically, and requires two boundary conditions. Assume that beyond a certain distance ρ_b quasineutrality will apply, i.e. the Laplacian term in (9) will be much smaller than either of the two terms on the right-hand side. The plasma solution is then

$$\rho \approx \frac{J^{1/2} e^{\phi/2}}{\phi^{1/4}}, \tag{10}$$

which is assumed to be true at ρ_b. For the second boundary condition, we take the derivative of $\phi(\rho)$ from (10), giving

$$\left[\frac{d\phi}{d\rho}\right]_{\rho_b} = \frac{2\rho_b}{J}\frac{\phi_b^{3/2}}{\phi_b - \frac{1}{2}} e^{-\phi_b}, \tag{11}$$

where ϕ_b is the value of ϕ at ρ_b. At the surface, substituting (6) into (5) gives

$$\frac{J}{P^2} = \alpha e^{-\Phi}, \tag{12}$$

where $\alpha = \sqrt{M_i/4\pi m_e}$ and $\Phi = \phi(P)$.

3. Finding an appropriate boundary condition

It has hitherto been known that the boundary condition must be set at sufficiently large radius in order to obtain a meaningful result. Here this criterion will be put into more concrete form. Obtain an expression for $(d/d\rho)(\rho^2 d\phi/d\rho)$ by differentiating the plasma solution. Only where this expression is small compared to $J\phi^{-1/2}$ will the plasma solution be valid. Thus the plasma condition is

$$\frac{4\phi(2\phi-3)(2\phi+1)}{(2\phi-1)^3} \ll \frac{J}{\phi^{1/2}},$$

https://doi.org/10.1017/S0022377802001691 Published online by Cambridge University Press

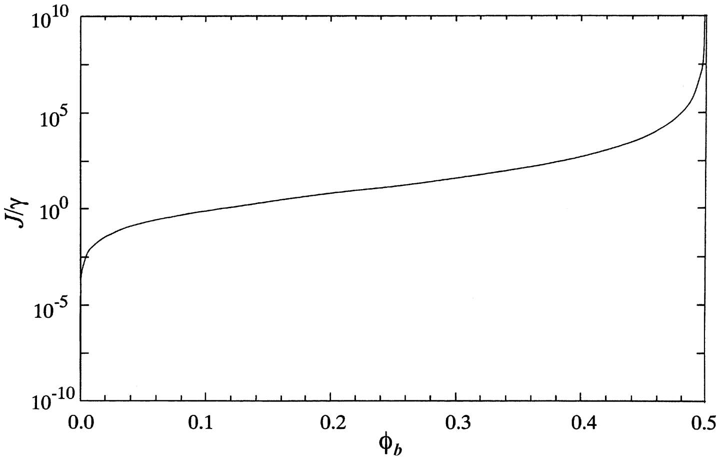

Figure 2. The plasma criterion. For a given current J, let γ be much greater than unity. The boundary potential ϕ_b is then taken from the curve.

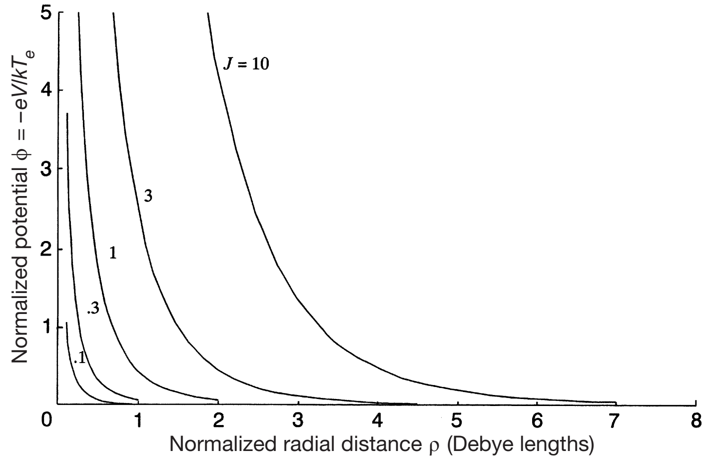

Figure 3. Potential around a spherical probe, for various values of the normalized ion current J (hydrogen plasma).

and an appropriate boundary value of ϕ is found from

$$\frac{J}{\gamma} = \frac{4\phi_b^{3/2}(2\phi_b - 3)(2\phi_b + 1)}{(2\phi_b - 1)^3}, \tag{13}$$

where γ is an arbitrary value, large compared with unity. The right-hand side of (13) is plotted in Fig. 2. We can now obtain results for potential distribution and floating potential by integrating (11) numerically from a boundary given by (10), (11) and (13). In such calculations, we specify J in advance, obtain a potential curve to arbitrarily small radii, and use the floating criterion to find the probe radius. Results are shown in Figs 3 and 4 for the potential distribution and floating potential respectively.

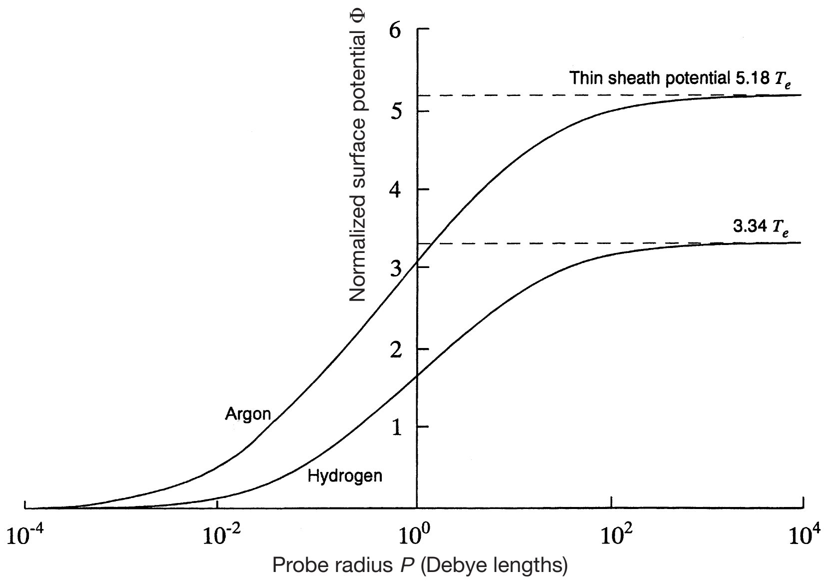

Figure 4. Probe floating potential $\Phi = -eV_p/kT_e$ plotted against probe radius $P = R/\lambda_D$ for hydrogen and argon.

4. Limit for small probes

For convenience, we switch to the logarithmic form:

$$\nu = \ln \phi, \qquad \psi = \ln \rho, \qquad K = \ln J, \tag{14}$$

and (9) becomes

$$\frac{d^2\nu}{d\psi^2} + \left(\frac{d\nu}{d\psi}\right)^2 + \frac{d\nu}{d\psi} = e^{K-\frac{3}{2}\nu} - e^{2\psi-\nu-e^{\nu}}. \tag{15}$$

Let

$$Y(\nu_b) = \ln\left(4\gamma \frac{(2e^{\nu_b}-3)(2e^{\nu_b}+1)}{(2e^{\nu_b}-1)^3}\right).$$

From (13), the boundary condition is now

$$K = \tfrac{3}{2}\nu_b + Y. \tag{16}$$

From (10),

$$\psi_b = \tfrac{1}{2}(\nu_b + Y + e^{\nu_b}) \tag{17}$$

and the floating criterion from (12) is

$$K - 2\psi_p = \ln \alpha - e^{\nu_p}. \tag{18}$$

Figure 5 shows the solutions to (15) for varying K, the function $\nu_p(\psi_p)$ from (18) and the locus of intersection between the two, which corresponds to the floating potential. Note that for very negative K the solutions appear to be congruent. This is demonstrated by changing the origin to (ψ_b, ν_b). Let $\zeta = \psi - \psi_b$ and $\upsilon = \nu - \nu_b$. Equation (15), using (16) and (17), becomes

$$\frac{d^2\upsilon}{d\zeta^2} + \left(\frac{d\upsilon}{d\zeta}\right)^2 + \frac{d\upsilon}{d\zeta} = e^{Y}(e^{-\frac{3}{2}\upsilon} - e^{e^{\nu_b}(1-e^{\upsilon})}e^{2\zeta-\upsilon}). \tag{19}$$

https://doi.org/10.1017/S0022377802001691 Published online by Cambridge University Press

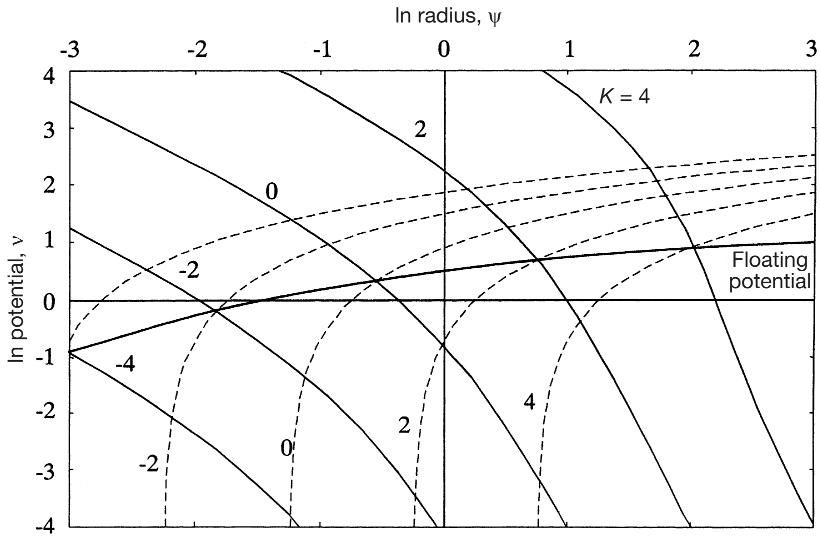

Figure 5. Logarithmic values of potential plotted against distance from probe centre (hydrogen plasma). The solid lines are potentials ν at position ψ, the dashed lines represent the floating criterion. Where the corresponding lines cross, $\psi = \psi_p$.

As we take more negative values of K, the limit of (16) gives $\nu_b \to \frac{2}{3}(K - \ln 12\gamma)$, i.e. ν_b also becomes highly negative. It will be shown later that in the limit of small probe radius, both ν_b and K tend to $-\infty$. In this limit, (19) reduces to

$$\frac{d^2\upsilon}{d\zeta^2} + \left(\frac{d\upsilon}{d\zeta}\right)^2 + \frac{d\upsilon}{d\zeta} = 12\gamma(e^{-\frac{3}{2}\upsilon} - e^{2\zeta-\upsilon}), \tag{20}$$

which is independent of K and ν_b and explains the congruent solutions (see Fig. 6). Equation (20) has two asymptotes. The limit of large positive ζ gives $\upsilon = -4\zeta$. The limit of large negative ζ is the so-called vacuum solution, which we obtain by assuming that υ increases as ζ decreases, thus making the right-hand side of (20) vanish in magnitude compared with the differential terms. Then it can easily be seen that a solution for $d\upsilon/d\zeta = -1$ exists and is consistent with the above assumptions. Thus

$$\lim_{\substack{\nu_b \to -\infty,\\ \zeta \to -\infty}} \upsilon = C - \zeta, \tag{21}$$

where C is a constant which depends on γ.

The floating criterion, from (16)–(18), is

$$e^{\upsilon_p} = e^{-\nu_b}(2\zeta_p - \tfrac{1}{2}\nu_b + \ln\alpha) + 1$$

As $\nu_b \to -\infty$, this gives

$$\lim_{\nu_b \to -\infty} \zeta_p = \tfrac{1}{4}\nu_b - \tfrac{1}{2}\ln\alpha, \tag{22}$$

i.e. $\zeta_p \to -\infty$, so we substitute (21) for υ into (22) to give

$$\lim_{\nu_b \to -\infty} \upsilon_p = C - \tfrac{1}{4}\nu_b + \tfrac{1}{2}\ln\alpha. \tag{23}$$

Now returning to $\{\nu, \psi\}$, (22) and (17) give the limit of ψ_p as

$$\lim_{\nu_b \to -\infty} \psi_p = \tfrac{3}{4}\nu_b + \tfrac{1}{2}\ln 12\gamma - \tfrac{1}{2}\ln\alpha;$$

https://doi.org/10.1017/S0022377802001691 Published online by Cambridge University Press

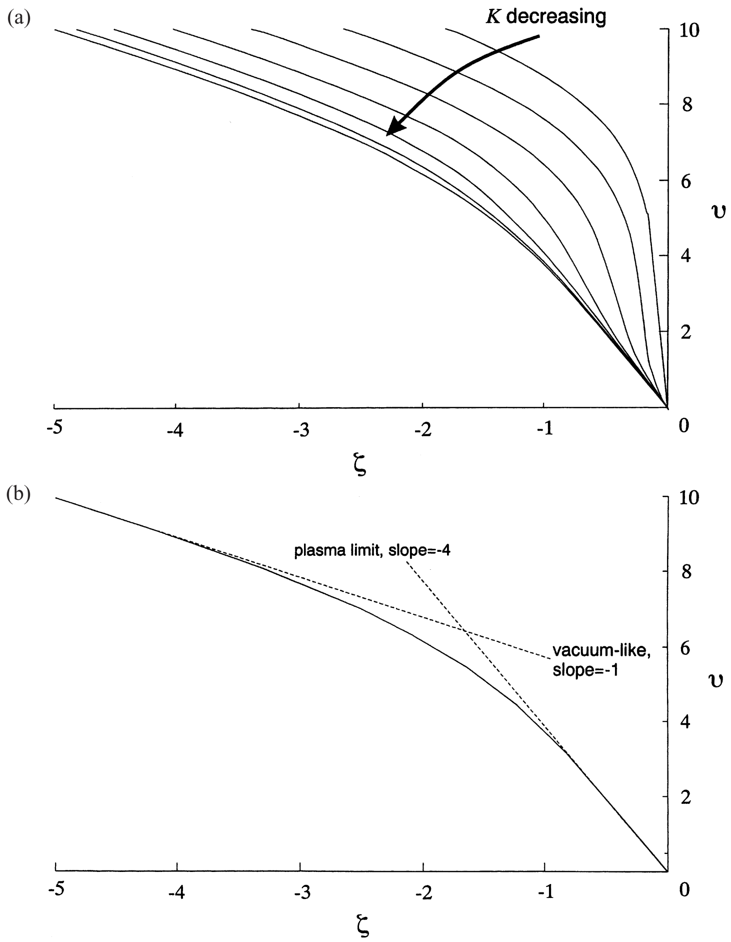

Figure 6. Solutions for the logarithmic potential, with $\gamma = 100$, for various values of K (hydrogen plasma).

so, as the probe radius tends to zero, $\nu_b \to -\infty$ (and, from (16), $K \to -\infty$). Now, from (23), we have the limit of ν_p as

$$\lim_{\nu_b \to -\infty} \nu_p = C + \tfrac{3}{4}\nu_b + \tfrac{1}{2}\ln\alpha, \tag{24}$$

i.e., for a given finite C, the limit of ν_p as $\psi_p \to -\infty$ is $-\infty$. This means, in our original notation,

$$\lim_{P \to 0} \Phi = 0. \tag{25}$$

It can be shown that the solution for any value of $\gamma > \gamma'$ lies beneath the solution for γ'. Thus (25) applies to the true solution, for which $\gamma \to \infty$.

5. Conclusions

To summarize, the limit of floating potential in the ABR radial theory as probe radius tends to zero is zero. If a cold-ion assumption is valid, the potential is strongly dependent on the probe radius for small and intermediate-sized probes, levelling

https://doi.org/10.1017/S0022377802001691 Published online by Cambridge University Press

out only for large probes. Dust grains are expected to reside in the lower regions of Fig. 4, where the probe radius is much smaller than the Debye length. This result is in contrast with the work of Nairn et al. (1998), who have potential levelling out at a finite value for small r/λ_D. This erroneous result was due to an inappropriate boundary condition. It has been established here that the plasma boundary in this theory is dependent on the size of the current, which in turn is a function of probe radius for floating probes. Further work on the theories that take finite ion temperature into account culminates in a complete set of floating potential data for relevant values of probe size and ion temperature.

References

Allen, J. E., Boyd, R. L. F. and Reynolds, P. 1957 The collection of positive ions by a probe immersed in a plasma. *Proc. Phys. Soc.* **B70**, 297–304.

Bernstein, I. B. and Rabinowitz, I. M. 1959 Theory of electrostatic probes in a low-density plasma. *Phys. Fluids* **2**, 112–121.

Bohm, D., Burhop, E. H. S. and Massey, H. S. W. 1949 The use of probes for plasma exploration in strong magnetic fields. In: *The Characteristics of Electrical Discharges in Magnetic Fields* (ed. A. Guthrie and R. K. Wakerling), New York: McGraw-Hill, pp. 13–76.

Bouchoule, A. (ed.) 1999 *Dusty Plasmas*. New York: Wiley, p. 366.

de Angelis, U. 1992 The physics of dusty plasmas. *Physica Scripta* **45**, 465–474.

Laframboise, J. G. 1966 The theory of spherical and cylindrical probes in a collisionless, Maxwellian plasma at rest. Institute for Aerospace Studies, University of Toronto (UTIAS) Report 100.

Nairn, C. M. C., Annaratone, B. M. and Allen, J. E. 1998 On the theory of spherical probes and dust grains. *Plasma Sources Sci. Technol.* **7**, 478–490.

Northrop, T. G. 1992 Dusty plasmas. *Physica Scripta* **45**, 475–490.